# Mechanistic Studies of Semicarbazone Triapine Targeting Human Ribonucleotide Reductase *in Vitro* and in Mammalian Cells: Tyrosyl Radical Quenching Not Involving Reactive Oxygen Species

## SUPPLEMENTAL TEXT

## CONTENTS

**MATERIALS AND METHODS.** All chemicals were purchased from Sigma in highest available purity and used without further purification. Triapine® (3-AP) was synthesized according to the published procedure (1) and stored as aliquots in DMSO at -80 °C. $NH_4^+$ salts of [5-$^3$H]-cytidine 5′-diphosphate (CDP, 17.0 Ci/mmol) was from Vitrax and $^{55}FeCl_3$ (2 mCi in 0.5 M HCl) was from Perkin Elmer. Bortezomib (Velcade®) was from LC Laboratories, MA. TALON® metal affinity resin was from Clontech. Dowex (50W-X4-200) was from Bio-RAD. Calf intestinal alkaline phosphatase (AP) (20 U/μL) and protease inhibitor tablets (Complete Mini, EDTA-free) were from Roche. Mouse monoclonal anti-human $\beta_2$ primary antibody (Ab57653) and anti-mouse secondary antibody (Ab6789) were from Abcam. Mouse monoclonal anti-GAPDH-peroxidase (G9295), apo-transferrin (T2036), RNAse A (R6513), propidium iodide (P4864), *B. subtilis* isocitrate dehydrogenase (94596), equine heart ferricytochrome C (C2506) and xanthine oxidase from bovine milk (X4376) were from Sigma. Bis(sulfosuccinimidyl)suberate (BS3) cross-linking reagent and enhanced chemiluminescent substrate were from Pierce. COS-1 and K562 cells were from American Type Culture Collection (ATCC). Hydroxyurea (HU)-resistant TA3 cells (2, 3) were a generous gift of Professor Lars Thelander (Professor Emeritus of the Department of Medical Biochemistry and Biophysics, Umeå University, Sweden). 1X TrypLE™ Express (stable trypsin-like enzyme with phenol red), 1X DMEM, 1X RPMI-1640, Dynabeads®-protein G and heat-inactivated horse serum (0.2 μm-filtered before use) were from Invitrogen. Fetal bovine serum (FBS) (0.2 μm-filtered) was from Hyclone. Oxyblot™ Protein Oxidation Detection Kit (S7150), ultrafiltration membranes (YM-30 and -10), Centricons, Minicons and Amicon Ultra centrifugal devices were from Millipore. *E. coli* thioredoxin [Trx, specific activity (SA) of 40 U/mg] and Trx reductase (TrxR, SA of 1800 U/mg), were isolated as previously described (4, 5). The extinction coefficients of 3-AP at pH 7.6, 1% DMSO in 50 mM Hepes was $\varepsilon_{368}$: 15600 $M^{-1}cm^{-1}$. Concentrations of recombinant proteins were determined using $\varepsilon_{280nm}/M^{-1}cm^{-1}$: 119160 and 45900 for hRNR α and β subunits, respectively (reported per monomer). Recombinant (r) N-terminal $His_6$-tagged hRNR subunits were expressed and purified [and in the case of β, subsequently reconstituted *in vitro*], as previously reported [SA's: 700-900 and 3000-4100 U/mg for r-$His_6$-α and –β, respectively, reported per monomer, where U is $nmolmin^{-1}$, and radical content at 0.9-1.2 Y•/$\beta_2$] (6-7). Aliquots of proteins stored at – 80 °C [typical storage (monomer) concentrations: 90-130 μM r-$His_6$-α and 50-120 μM r-$His_6$-β] were designated for single-use only, without any further freeze-thaw. Storage buffers contained 50 mM Tris (pH 7.6), 100 mM KCl and 5% glycerol for r-$His_6$-β. 5 mM DTT and 15 mM $MgCl_2$ were additionally included in the case of r-$His_6$-α. Concentrations of apo- and holo-transferrin were determined using $\varepsilon_{280nm}/M^{-1}cm^{-1}$: 90000 and 110000, respectively (8). Concentrations of total proteins in lysate were estimated by Bradford assay using either BSA or IgG as standard (9). Chill-out wax and PVDF

membranes were from Bio-Rad. Density analyses of the bands from western blots and silver-stained SDS-PAGE were performed using Quantity-One software from Bio-Rad. Cell counting was either performed on a Coulter Z1 particle counter™, or using a hemacytometer under light microscope for trypan blue dye exclusion test. Olympus CKX31 and Olympus IX50 were used for light microscopy. Fluorescence-activated cell sorting (FACS) was performed on a FACSCalibur flow cytometer. EPR spectra acquisition procedures are detailed in relevant experimental sections. Curve fitting and data analyses were performed using GraphPad PRISM Version 5.0 (GraphPad software Inc., CA), KaleidaGraph Version 4.03 (Synergy Software, PA). FACS data and mass spectrometry data analyses of in gel trypsin-digested $\beta_2$ were carried out, respectively, using FlowJo (version 7.6.4) and Scaffold 3.5Q+ (Proteome software, OR).

**1) Time-Dependent Assays for the Loss of Subunit-Specific Activity (Fig. 2A).**

A typical inhibition mixture in 150 μL contained: 0.6 μM (r-$His_6$-$\beta$)$_2$ (3400 U/mg of $\beta$, 1.2 Y•/$\beta_2$), 3-AP (0.3, 1.2 or 6.0 μM) or vehicle (appropriate % DMSO in $ddH_2O$), KCl (100 mM), in 50 mM Hepes (pH 7.6). The mixture was preincubated for 2 min at 37 $^oC$. The reaction was initiated by the addition of 3-AP or vehicle. Aliquots were removed at indicated time points and diluted 4-fold into assay mixture precubated at 37 $^oC$. The assay mixture for each time point contained in a final volume of 40 μL: 1.1 μM (r-$His_6$-$\alpha$)$_2$ (892 U/mg of $\alpha$), 100 μM Trx, 1 μM TrxR, 2 mM NADPH, 3 mM ATP, 15 mM $MgCl_2$, 1.0 mM [5-$^3$H]-CDP, 100 mM KCl, in 50 mM Hepes (pH 7.6)]. The reaction was allowed to proceed for 3 min and quenched with 2% $HClO_4$, followed immediately by neutralization with 0.4 M KOH at 4 $^oC$. Control samples with vehicle in place of 3-AP were run under identical conditions to monitor intrinsic activity loss. $\alpha_2$ activity in the presence of 3-AP was identical to control experiments. $\beta_2$ activity decay shown in Fig. 2A has been corrected for inherent activity depletion under assay conditions.

**2) Active site $^{55}$Fe labeling.**

**Reconstitution protocol Using Fe(III).**

In a glove box, 50 mM $^{55}FeCl_3$ stock solution (pH 6.8) was prepared to 1240 cpm/nmol of Fe, by mixing appropriate amounts of $^{55}FeCl_3$ stock (Perkin Elmer) with $FeCl_3.6H_2O$ in 50 mM Hepes (pH 7.6). $^{55}$Fe(II) solution was then prepared in the glove box. In a final volume of 1 mL, the reaction mixture contained in final concentrations: 500 μM of $^{55}FeCl_3$, 1 mM DTT and 50 mM Hepes (pH 7.6). The reaction was incubated at 37 $^oC$ for 3 h at which point the reaction was judged complete by a ferrozine assay (10). The resulting $^{55}$Fe(II) solution stored at 4 $^oC$ in the glove box was found to be stable and reusable for at least 2 weeks.

An Ar-saturated solution (624 μL) contained: 22 μM recombinant (r)-(apo-$\beta$)$_2$ (14 nmol $\beta_2$) (7), 50 mM Tris (pH 7.6), 100 mM KCl and 10% glycerol was brought into the glove box. $^{55}$Fe(II) stock solution (112 nmol, 222 μL) was added and the mixture incubated at 37 $^{o}$C for 4 min. Subsequent to removal of the sample from the glove box, 168 μL of $O_2$-saturated storage buffer [50 mM Tris (pH 7.6), 100 mM KCl and 5% glycerol] was added. All steps hereafter were carried out at 4 $^{o}$C. The sample was loaded onto a pre-equilibrated Sephadex G-25 column (1.5 cm x 5 cm). The labeled protein was concentrated to 50-120 μM. Protein subsequently used in experiments underwent a single freeze-thaw. The procedure afforded [($Fe^{III}_2$-Y•)($Fe^{III}_2$)]-$\beta_2$ (SA: 1173 cpm/nmol of $\beta$). Radical content, specific activity and Fe-content of the labeled protein were similar to $\beta_2$ reconstituted using $Fe(NH_4)_2(SO_4)_2$ (6, 7).

A typical reconstitution gave, 0.9-1.2 Y•/$\beta_2$ and the non-specifically surface-bound $Fe^{III}$ (estimated by *g*=4.3) (11-12) was less than 5% (<0.18Fe/$\beta_2$). Spin quantitation was made, according to published procedure (12). Ferrozine assay gave 3.2-3.6 Fe/$\beta_2$ (10). Specific activity of $\beta_2$ reconstituted using using unlabeled $FeCl_3$, was 3000-4100 U/mg of $\beta$.

Studies on the untagged-$\beta_2$, gave results identifical to the $His_6$-tag on $\beta_2$. All *in vitro* experiments thus used tagged-$\beta_2$.

**Analysis of the Rate of Active Site Fe Loss (Fig. 2B-D)**

The reaction mixture at 37 $^{o}$C contained in a final volume of 3.7 mL: 1 μM $^{55}$Fe-labeled (r)-($His_6$-$\beta$)$_2$ and 10 μM 3-AP or vehicle (5 % of DMSO in dd$H_2O$). For the analysis of Fe loss on $\beta_2$ alone (Fig. 2B), the reaction was carried out in storage buffer [100 mM KCl, 50 mM Tris (pH 7.6), 5% glycerol]. For non-cycling holo-complex (Fig. 2C), 1 μM (r-$His_6$-$\alpha$)$_2$, 3 mM ATP and 15 mM $MgCl_2$ were additionally present. For cycling holo-complex (Fig. 2D), the reducing system of 100 μM Trx, 1 μM TrxR, 2 μM NADPH was added with substrate (1 mM CDP), and assay buffer [50 mM Hepes (pH 7.6)] replaced storage buffer. No difference was observed between the storage buffer or assay buffer for the rate of Fe loss in the cycling holo-complex.

The reaction minus [$^{55}$Fe]-$\beta_2$ was pre-warmed at 37 $^{o}$C for 2 min and initiated with [$^{55}$Fe]- $\beta_2$. At indicated time points, 270 μL aliquots were removed, and 135 μL was added to two pre-chilled (4 $^{o}$C) YM-30 mini ultrafiltration membranes (Millipore) that had been pre-equilibrated with the reaction buffer. Centrifugation was carried out at 6000 x g at 1 $^{o}$C over 3 min. Combined flow-through from the two tubes (2 x 80 μL) was diluted to 1 mL with the reaction buffer and analyzed by liquid scintillation counting. Radioactivity associated with the volume retained within the membrane in each time point was accounted for in the data sets presented. Background in each case was determined from the aliquot removed prior to initiating the reaction with labeled $\beta_2$.

**3) Time-Dependent Assays for the Loss of Y•.**

***$\beta_2$ alone under aerobic conditions (Fig. 2E and S1)***

*Experiments with 3-AP or its Fe-chelates:*

The inhibition mixture in a final volume of 1.3 mL contained: 5 μM (r-$His_6$-β)$_2$ (3400 U/mg of β at 1.2 Y•/$\beta_2$), 50 μM 3-AP alone, or 50 μM Fe(III)-(3-AP) (freshly prepared from 50 μM 3-AP + 50 μM $FeCl_3$), or 3 or 50 μM Fe(II)-(3-AP) (freshly prepared from 3 or 50 μM 3-AP + 3 or 50 μM $FeCl_3$ and either 5 mM GSH or 5 mM DTT), or vehicle (DMSO), 100 mM KCl and 50 mM Hepes (pH 7.6). The mixture without 3-AP or DMSO was pre-warmed at 37 $^oC$ for 0.5 min and initiated by addition of the appropriate inhibitor or its Fe-chelate. At designated time points, 250 μL aliquots were placed into EPR tubes at 4 $^oC$, and the samples immediately flash-frozen in liq $N_2$. Control samples were treated under identical conditions except that DMSO replaced 3-AP. All data shown in Fig. 2E have been adjusted for intrinsic decay from control experiments.

*Experiments with $H_2O_2$ and $O_2$•$^-$:*

With $H_2O_2$: The reaction mixture, in a final volume of 0.8 mL contained: 5 μM (r-$His_6$-β)$_2$ (3400 U/mg of β at 1.2 Y•/$\beta_2$), 100 mM KCl, 50 mM Hepes (pH 7.6), either 50 μM or 0.5 mM $H_2O_2$. Control experiments have dd$H_2O$ in place of $H_2O_2$. The mixture was pre-warmed at 37 $^oC$ for 0.5 min and initiated by addition of $H_2O_2$ or dd$H_2O$. At designated time points, 250 μL aliquots were placed in EPR tubes that had been pre-chilled at 4 $^oC$ and the samples were immediately flash-frozen in liq $N_2$.

With $O_2$•$^-$: Superoxide generated from xanthine (X)/xanthine oxidase (XO) system replaced $H_2O_2$ above. Final concentrations/amounts of X/XO employed were either 46 μM /14 mU or 653 μM /196 mU. Steady-state generation of $O_2$•$^-$ was independently determined according to published protocols (13-16) using ferricytochrome C reduction assays (14-15). Two sets of control experiments were performed, one without X in an otherwise complete reaction mixture with 196 mU of XO, or without XO but with 653 μM X. Controls showed that neither X nor XO affects the stability of Y•.

***Holo-complex under aerobic conditions (Fig. S1B)***

The procedure was identical to (r-$His_6$-β)$_2$ alone above except that 5 μM (r-$His_6$-α)$_2$ and 3 mM ATP were additionally present.

***$\beta_2$ alone under anaerobic conditions (Fig. 2E)***

All reaction components (3-AP, Argon-saturated DMSO, degassed buffer solutions) and hardware were left in vacuo overnight, except the protein that was degassed on a Schlenk line (6), were brought into the glove box, and stored at 4 $^oC$ until. All the remaining steps of the experiment were carried out in the glove box. The inhibition mixture in a final volume of 1.3 mL contained: 5 μM (r-$His_6$-

$\beta)_2$ (3400 U/mg of β, 1.2 Y•/$\beta_2$), 50 μM Fe(II)-(3-AP) [freshly prepared in the glove box from 50 μM 3-AP + 50 μM $Fe(NH_4)_2(SO_4)_2$], or Fe(III)-(3-AP) (freshly prepared from 50 μM 3-AP + 50 μM $FeCl_3$) ± 5 mM GSH, or vehicle, and 50 mM Hepes (pH 7.6). The mixture without pre-complexed [Fe(II)-(3-AP)] or [Fe(III)-(3-AP)] or DMSO was pre-warmed at 37 $^oC$ for 2 min, and initiated by addition of [Fe(II)-(3-AP)], [Fe(III)-(3-AP)] or DMSO. At designated time points, 250 μL aliquots were placed into EPR tubes at 4 $^oC$ and the samples immediately flash-frozen in liq $N_2$. Corresponding control samples were treated under identical conditions except that DMSO/$H_2O$ replaced 3-AP.

**4) Cell Culture and Cell Lifting Protocols.**

All cells were cultured at 37 $^oC$ under 5% $CO_2$ atmosphere. The media used were either RPMI-1640 (K562) or DMEM (TA3 and COS-1) supplemented with 10% either FBS (K562 and COS-1) or Horse serum (TA3), except in the $^{55}Fe$ pulse labeling experiments where amount of FBS was lowered to 1%. In K562 cells, media were changed 24 h prior to all experiments to ensure that cells were in exponential growth. For adherent cells (TA3 and COS-1), experiments were conducted when the cells reached 70-80% confluence. TA3 cell lines were maintained and passaged in the presence of 2 mM HU (2, 3), and the HU containing media was changed daily. HU was removed 24-36 h prior to all experiments. During experiments, 3-AP containing media was freshly prepared by adding 3-AP from a stock solution in 100% DMSO. Where applicable, CHX solution in DMSO was freshly prepared. At the end of the indicated incubation periods, cells were tyrpsinized (for TA3 and COS-1 only); spun down (500 x g for 5 min at 4 $^oC$) and washed first with 1 X PBS, followed by a second wash with 50 mM Hepes (pH 7.6). Cell counting was performed using Coulter Multisizer$^{TM}$ according to the manufacturer's protocol.

**5) Cell Viability Analysis (Fig. S3).**

The procedure was identical to that previously reported (19).

**6) Cell Cycle Progression Analysis by Fluorescence-Activated Cell Sorting (FACS) (Fig. S4).**

An analogous procedure to that previously described was performed (19). Data analysis was carried out using FlowJo (version 7.6.4).

**7) EPR Sample Preparation and Analysis.**

***In Vitro for the Detection of Y• (Fig. 2E, S1A and S6B)***

EPR spectra of Y• reconstituted *in vitro* were acquired at 77 K on a Brüker EMX X-band spectrometer (9.3 GHz, 1.0 mW power, 3.17 x $10^4$ gain, 1.0-G modulation amplitude). The concentration

of Y• was obtained by comparing the double integral with a $CuSO_4$ standard solution (1 mM Cu, 10 mM EDTA) (11). All analyses were performed using Win-EPR software (Brüker).

***In Vitro for the Surface-Bound S=5/2 Fe(III) (g=4.3)***

Sample preparation and analysis of the Fe(III)-EDTA standard solution were carried out as previously described (12). Spectra for the estimation of the amount of non-specific surface bound Fe in $[(Fe^{III}_2\text{-}Y\bullet)(Fe^{III}_2)]\text{-}\beta_2$ were acquired at 77 K on a Brüker EMX X-band spectrometer (9.3 GHz, 0.27 mW power, 60 dB receiver gain, 10.0 G modulation amplitude) and analysis was performed using Win-EPR software (Brüker).

***In Intact Mammalian Cells for the Detection of Endogenous Y• (Fig. 3B, S6A, C and D)***

Previously reported protocols were modified (2, 3, 17). Subsequent to washing with 1 X PBS, cells were re-suspended in 50 mM Hepes (pH 7.6) including 5% glycerol, and transferred to an EPR tube. The tube was spun down at 50 x g for 5 min at 4 $^oC$. Supernatant was removed and the remaining ~200 μL of packed cells were rapidly (<5 s) frozen stepwise [first in MeOH pre-chilled over dry ice at ~ -70 $^oC$, followed by liq $N_2$]. Cells were stored in liq $N_2$ and analyzed using a Bruker EMX X-band spectrometer (9.3 GHz, 3.17 x $10^4$ gain) and a liq $N_2$ finger-dewar (77 K analysis) or an Oxford Instruments ESR-900 helium cryostat (set at 30 K). Each tube contained ~ 80 million packed cells (as judged by Coulter Multisizer$^{TM}$ cell counting). All spectra were recorded under non-saturating conditions: 0.5 or 2.0 mW for TA3 and K562 cells, respectively. Modulation amplitudes were 2.5 and 5 G for TA3 and K562 cells. It has been previously reported that electron-spin relaxation properties of the human and mouse enzymes render the signal resistant to power-saturation, allowing spin-quantitation at high microware powers (2-3, 17). Note that the source of apparent background signals in K562 (Fig. S6D) was previously discussed (17-18). Spectra analyses were performed using Win-EPR software (Brüker).

**8) Cell Lysis Protocol.**

Subsequent to harvest (detailed in 'Cell culture and cell lifting protocols' above), each pellet, was lysed according to previously published protocols (19). The supernatant was used immediately.

**9) Lysate Activity Assays (Fig. 3A and S5).**

The $\alpha_2$-subunit activity for CDP reduction was determined as recently reported (1) using the method of Steeper and Steuart (20).

**10) Western Blot of Cell Lysates (Fig. 3C, 4, 5A, 6A and S7).**

Western blotting was carried out as previously reported (19). Abcam Ab57653 and Ab6789 was used as primary and secondary Abs respectively at 1:2000 dilutions. Where applicable, standard curves were generated using r-$His_6$-β (25-250 ng, monomer, 47 kDa). For loading controls, membranes were re-probed with mouse monoclonal anti-GAPDH-peroxidase (1:30000 dilution) (monomer, 37 kDa) (Sigma).

**11) Assessment of Protein Carbonylation *in Vitro* and in Crude Lysates (Fig. S2).**

Western blot analysis for protein carbonylation was performed according to the manufacturer's protocol (Millipore Oxyblot Kit™). Briefly, all carbonyl groups present in either *in vitro* samples or mammalian lysates, were derivatized by dinitrophenyl hydrazine (DNPH) for 15 min at room temperature, after which the reaction was stopped by the addition of neutralization solution provided in the kit. Positive control samples for oxidized $b_2$ were obtained according to the manufacture's protocol. Briefly, 2-5 mg/mL (r-β)$_2$ was treated with 25 mM ascorbate, 100 μM $FeCl_3$ in 25 mM Hepes (pH 7.2), incubated at 37 $^oC$ for 5 h, dialyzed against 50 mM Hepes, pH 7.6 and 1 mM EDTA, and the carbonyls derivatized by DNPH as above. All samples were loaded directly onto the gels for SDS-PAGE and subsequent western blot analyses.

**12) Proteasomal Degradation Assays (Fig. 4A).**

Cell pellets were diluted into lysis buffer specific [250 mM sucrose, 50 mM $KP_i$ (pH 7.8), 1 mM KCl and 10 mM $MgCl_2$, and 0.5 mM βME]. Cells were lysed in a dounce homogenizer at 4 $^oC$ (10 strokes) then the lysate was centrifuged at 12000 x g. Protein concentration was measured in lysate using Bradford analysis relative to IgG (Bio-Rad). The stock lysate was diluted to 10 mg/mL or 1 mg/mL with lysis buffer. The lysate was supplemented with an ATP regenerating system consisting of 10 mM ATP, 270 mM $MgCl_2$ and 94 mM creatine phosphate. Apo-$\beta_2$ or [($Fe^{III}_2$-Y•)($Fe^{III}_2$)]-$\beta_2$ (holo-$\beta_2$) were added to the lysate on ice to a final concentration of 1 mg per 15 μL. Immediately after this addition, a 15 μL aliquot was removed from each reaction tube and added to 7 μL 5X Lamelli buffer to obtain the zero time point. Reaction tubes were then overlayed with Chill-Out wax (Bio-Rad) and heated to 37 $^oC$ in a PCR machine with the lid set to 37 $^oC$. At subsequent time points, 15 mL aliquots were removed from the reaction and quenched with 7 μL 5X Laemeli loading buffer. As a control, in separate sets of experiments, bortezomib (Velcade®) (30 μM) was also added to the lysates 10 min prior to addition of the exogenous apo-$\beta_2$ or holo-$\beta_2$. All lysates were incubated on ice throughout the 10-min bortezomib incubation time.

**13) Assessment of Protein Stability using Cycloheximide (CHX)-Treated Cells (Fig. 5).**

COS-1 cells were cultured in 16 x 25 $cm^2$ plates. At ~80% confluency (~ $7x10^6$ million cells/plate), 8 of the plates (plates 1-8) were treated with CHX (0.2 mg/mL) and the other 8 plates (9-16) with DMSO for 30 min. Cells from plates 1-4 and 9-12 were exchanged with fresh media containing 3-AP (5 μM) and either fresh CHX (for plates 1-4) or DMSO (for plates 9-12) (this set is called the **3-AP set**). In parallel, cells from plates 5-8 and 13-16 were exchanged with fresh media with no 3-AP, but were retreated with either CHX (for plates 5-8) or DMSO (for plates 13-16) (this set is called the **NO 3-AP set**). All cells were incubated for a further 3 h, after which time, cells were trypsinized and pelleted. The resulting cells were lysed and analyzed for $\beta_2$ and GAPDH (loading control) by western blot. The averaged intensity of the $\beta_2$ signal from the CHX-treated cells for each set was then divided by the equiv signal for the DMSO-treated cells for each set. This comparison [(CHX **3-AP set**)/(DMSO **3-AP set**)] vs. [(CHX **NO 3-AP set**)/ (DMSO **NO 3-AP set**)] represents the relative effect (labeled in Fig 5. as CHX+3-AP) and (labeled as CHX) respectively has on the cells (Fig. 5).

**14) Preparation of [$^{55}$Fe]-Human Transferrin (Tf).**

Tf was labeled with $^{55}$Fe by a modification of the previously reported methods (21-22).

**15) $^{55}$Fe Pulse Labeling of Mammalian Cells (Fig. 6).**

K562 cells grown in RPMI containing 5% FBS were centrifuged at 500 x g for 5 min (rt) and washed three times with pre-warmed (37 $^oC$) 1X PBS. The cells (ca. $2x10^6$/mL) were resuspended in RPMI supplemented with 1% FBS, and incubated with $^{55}$Fe-Tf (SA: 238900 cpm/nmol) to a final concentration of 25 μg/mL at 37 $^oC$ for 18 h under 5% $CO_2$ atmosphere. The samples were centrifuged (500 x g, 5 min, rt), washed twice with 1X PBS (37 $^oC$), and resuspended in 1% FBS in RPMI in the presence and absence of 5 μM 3-AP. After incubation for 30 min at 37 $^oC$ under 5% $CO_2$ atmosphere, the cells were harvested. Using liquid scintillation counting, the amount of $^{55}$Fe in the supernatant and each wash in all steps was measured prior to immunoprecipitation.

**16) Immunoprecipitation (IP) of $\beta_2$ from Mammalian Cells (Fig. 6).**

Protein G-dyna magnetic beads (Invitrogen) were conjugated with monoclonal anti-hRNR-$\beta_2$ antibody (Abcam, Ab57653) using BS3 crosslinker (Invitrogen) according to the manufacturer's protocol. K562 cells (~ 80 x $10^6$, $^{55}$Fe-pulse-labeled/unlabeled &/or 3-AP-treated/untreated) were resuspended in 550 μL lysis buffer specific for IP [50 mM Hepes (pH 7.6), 10 mM NaF, 500 mM NaCl, 5 mM BME, 0.01% Tween, Roche protease inhibitor cocktail (1 tablet/5 mL)] and lysed via 3 cycles of flash-freeze-thaw. Binding: 500 μL of lysate was incubated with anti-$\beta_2$-cross-linked-protein-G-dynabeads at rt for 5

min. Wash: The beads were washed 3X with 600 μL wash buffer [50 mM Hepes (pH 7.6), 500 mM NaCl, 5 mM BME, 0.01% Tween] for 2 min incubation at rt. Elution: 10 μL of 2X Lamelli sample buffer containing 3% BME and 10 μL of wash buffer were added to the beads. The suspension was heated at 65 $^{o}$C for 10 min and the supernatant was collected. In pulse-labeling experiments, the entire supernatant from each step was analyzed by liquid scintillation counting. As a control for specificity and for the determination of background, identical IP experiments were carried out where buffer replaced anti-$\beta_2$ antibody but protein G-dyna beads were kept. In the positive control for Fe loss induced by HU, identical sets of IPs were carried out wherein 10 mM HU or water was added to the lysate prior to incubation with the beads.

**17) Mammalian Aconitase Lysate Activity Assays.**

COS cells stored at -80 $^{o}$C under Ar were brought into an anaerobic chamber and subjected to three freeze-thaw cycles in degassed lysis buffer [25 mM Tris (pH 7.5), 40 mM KCl, 2% Triton X-100, 0.6 mM $MnCl_2$, 2 mM citric acid, 5 mM DTT, 1 mM AEBSF and Complete$^{TM}$ EDTA free protease inhibitor cocktail (2 tablets/mL)]. Total mammalian aconitase activity in the resultant lysate was measured as described (23-24). Mitochondrial and cytosolic aconitases have been reported to contribute approximately equally to the measured total (25).

**18) Digest Mass Spectrometry Analysis of $\beta_2$ Inhibited *in vitro* (Table S1).**

(r-$His_6$-$\beta$)$_2$ (5 μM) in 100 mM KCl and 50 mM Hepes (pH 7.6) at 37 $^{o}$C was treated either with 5 equiv (per $\beta$) of pre-assembled Fe(II)-(3-AP) (freshly prepared by treatment of 50 μM $FeCl_3$ and 50 μM 3-AP with 5 mM GSH) (Table S1, Sample 1) or 5 equiv (per $\beta$) of $H_2O_2$ (Sample 2; note this does not lead to $\beta_2$ inhibition, see Fig 2E). DMSO replaced Fe(III)-(3-AP)/GSH or $H_2O_2$ in the Control sample. After 20 min incubation, the samples were quenched with Laemelli buffer and analyzed by 10% SDS-PAGE. Protein bands were excised from gels and were processed following published procedures (26). Briefly, after extensive washings to remove the protein Coomassie stain and SDS, protein disulfides were reduced with DTT and cysteines were alkylated with iodoacetamide. In-gel digestions were carried out overnight at room temperature using trypsin (Promega). Proteolytic peptides were extracted from the gel pieces with several extractions using a 1:1 mixture of water and acetonitrile acidified with 0.5% formic acids. The volume was reduced and the acetonitrile was removed in a vacuum centrifuge (Eppendorf). Proteolytic peptides were analyzed by HPLC and mass spectrometry. A nanoflow HPLC system (Agilent) with gradient elution, using a water-acetonitrile solvent system with 0.1% formic acid as the ion-pairing agent, was used to effect peptide separation on a 25 cm long reversed phase $C_{18}$ capillary column (75 mm internal diameter "PicoFrit", New Objective, Inc.) at a flow rate of 280 nL/min. Electrospray ionization

mass spectrometry was carried out on an LTQ ion trap mass spectrometer (ThermoFisher). The molecular mass data and fragment ion mass spectra that were collected for proteolytic peptides were used to search the SwissProt protein database using the Mascot database search software (Matrix Science). Oxidation of methionine and of tryptophan were specified as variable modifications. The protein identification results were tabulated using the Scaffold software (Proteome Software). All assignments were confirmed by careful examination of the corresponding fragment ion mass spectra.

**Supplemental References**

(1) Kowol, C. R., Trondl, R., Heffeter, P., Arion, V. B., Jakupec, M. A., Roller, A., Galanski, M., Berger, W. and Keppler, B. K. (2009) Impact of Metal Coordination on Cytotoxicity of 3-Aminopyridine-2-carboxaldehyde Thiosemicarbazone (Triapine) and Novel Insights into Terminal Dimethylation. *J. Med. Chem.* **52,** 5032-5043.

(2) Eriksson, S., Gräslund, A., Skog, S., Thelander, L., and Tribukait, B. (1984) Cell cycle-dependent regulation of mammalian ribonucleotide reductase. The S-phase correlated increase in subunit M2 is regulated by de novo protein synthesis. *J. Biol. Chem.* **259,** 11695-11700.

(3) Nyholm, S., Mann, G. J., Johansson, A. G., Bergeron, R. J., Gräslund, A., and Thelander, M. (1993) Role of ribonucleotide reductase in inhibition of mammalian cell growth by potent iron chelators. *J. Biol. Chem.* **268,** 26200-26205.

(4) Lunn, C.A., Kathju, S., Wallace, B.J., Kushnern, S.R., and Pigiet, V. (1984) Amplification and purification of plasmid-encoded thioredoxin from *Escherichia coli* K12. *J. Biol. Chem.* **259,** 10469–10474.

(5) Pigiet, V. P., and Conley, R. R. (1977) Purification of thioredoxin, thioredoxin reductase, and glutathione reductase by affinity chromatography. *J. Biol. Chem* **252,** 6367–6372.

(6) Wang, J., Lohman, G. J. S., and Stubbe J. (2007) Enhanced subunit interactions with gemcitabine-5´-diphosphate inhibit ribonucleotide reductases. *Proc. Natl. Acad. Sci. USA* **104,** 14324-14329.

(7) Aye, Y., and Stubbe, J. (2011) Clofarabine 5´-di and –triphosphates inhibit human ribonucleotide reductase by altering the quaternary structure of its large subunit. *Proc. Natl. Acad. Sci. USA* **108,** 9815-9820.

(8) Teeters, C. L., Lodish, H. F., Ciechanover, A., and Wallace, B. A. (1986) Transferrin and apotransferrin: pH-dependent conformational changes associated with receptor-mediated uptake. *Ann. N. Y. Acad. Sci.* 403-407.

(9) Bradford, M. (1976) A rapid and sensitive method for the quantitation of microgram quantitites of protein utilizing the principle of protein-dye binding. *Anal. Biochem.* **72,** 248-254.

(10) Fish W. W. (1988) Rapid colorimetric micromethod for the quantitation of complexed iron in biological samples. *Methods Enzymol*. **158,** 357–364.

(11) Aasa, R., and Vanngard, T. (1975) EPR signal intensity and powder shapes: a reexamination. *J. Magn. Reson.* **19,** 308-315.

(12) Bou-Abdallah, F., and Chasteen, N. D. (2008) Spin concentration measurements of high-spin (g = 4.3) rhombic iron(III) ions in biological samples: theory and application. *J. Biol. Inorg. Chem.* **13,** 15-24.

(13) McCord, J. M., and Fridovich, I. (1969) Superoxide dismutase. An enzymatic function for erythrocuprein (hemocuprein), *J. Biol. Chem.* **244,** 6049-6055.

(14) Del Maestro, R. F., Bjork, J., and Arfors, K-E. (1981) Increase in microvascular permeability induced by enzymatically generated free radicals. *Microvascular Res.* **22,** 239-254.

(15) Van Gelder, B. F., and Slater, E. C. (1962) The extinction coefficient of cytochrome *c, Biochim. Biophys. Acta* **58,** 593-595.

(16) Imaly, J. A., and Fridovich, I. (1991) Assay of metabolic superoxide production in *Escherichia coli*. *J. Biol. Chem.* **266,** 6957-6965.

(17) Cooper, C. E., Lynagh, G. R., Hoyes, K. P., Hider, R. C., Cammack, R., and Porter, J. B. (1996) The relationship of intracellular iron chelation to the inhibition and regulation of human ribonuleotide reductase. *J. Biol. Chem.* **271,** 20291-20299.

(18) Cammack, R. (1988) Electron paramagnetic resonance characterization of iron-sulfur proteins. *Methods Enzymol*, **167,** 427-436.

(19) Aye, Y., Brignole, E. J., Long, M. J. C., Chittuluru, J., Drennan, C. L., Asturias, F. J. and Stubbe, J. (2012) Clofarabine targets the large subunit ($\alpha$) of human ribonucleotide reductase in live cells by assembly into persistent hexamers. *Chem. Biol.* **19**, 799-805.

(20) Steeper, J. R., and Steuart, C. C. (1970) A rapid assay for CDP reductase activity in mammalian cell extracts. *Anal. Biochem.* **34,** 123-130.

(21) Klausner, R. D., van Renswoude, J., Ashwell, G., Kempf, C., Schechter, A. N., Dean, A., and Bridges, K. R. (1983) Receptor-mediated endocytosis of transferrin in K562 cells. *J. Biol. Chem.* **258,** 4715-4724.

(22) Fuller, S. D., and Simons, K. (1986) Transferrin receptor polarity and recycling accuracy in 'tight' and 'leaky' strains of Madin-Darby canine kidney cells. *J. Cell. Biol*. **103,** 1767-1779.

(23) Rose, I. A., and O'Connell, E. L. (1967) Mechanism of aconitase action. *J. Biol. Chem.* **242,** 1870-1879.

(24) Meyron-Holtz, E. G., Ghosh, M. C., Iwai, K., LaVaute, T., Brazzolotto, X., Berger, U. V., Land, W., Ollivierre-Wilson, H., Grinberg, A., Love, P. and Rouault, T. A. (2004) Genetic ablations of iron regulatory proteins 1 and 2 reveal why iron regulatory protein 2 dominates iron homeostasis. *EMBO J.* **23,** 386-395.

(25) See, for example, Kennedy, M. C., Mende-Mueller, L., Blondin, G. A., and Beinert, H. (1992) Purification and characterization of cytosolic aconitase from beef liver and its relationship to the iron-responsive element binding protein. *Proc. Natl. Acad. Sci. USA* **89,** 11730-11734.

(26) Shevchenko, A., Tomas, H., Havlis, J., Olsen, J. V., and Mann, M. (2006) In-gel digestion for mass spectrometric characterization of proteins and proteomes. *Nat. Protoc.* **1,** 2856-2860.

Mechanistic Studies of Triapine Targeting Human Ribonucleotide Reductase *in Vitro* and in Mammalian Cells: Tyrosyl Radical Quenching Not Involving ROS

**SUPPLEMENTAL FIGURES AND TABLES**

**CONTENTS**

**SUPPORTING FIGURES**

**Figure S1.**

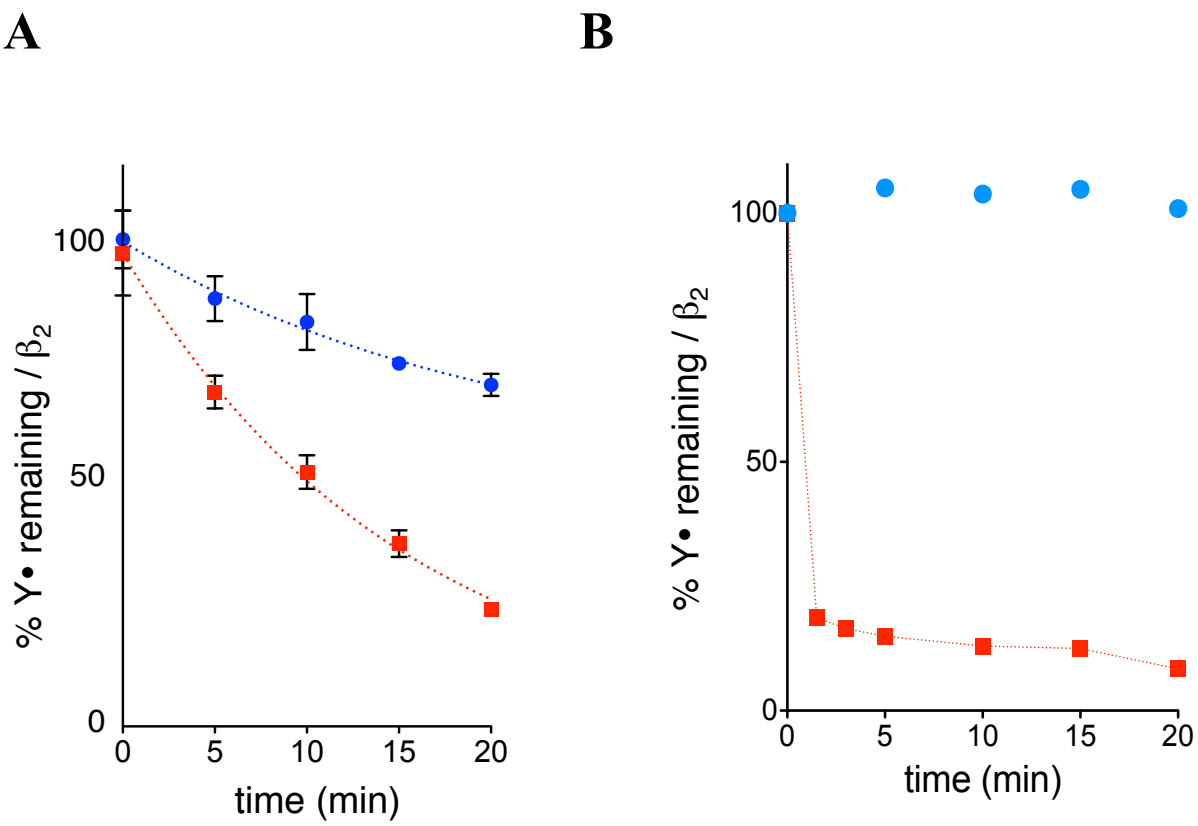


**Figure. S1.** *In Vitro* EPR analysis of effects of 3-AP on Y• loss in $\beta_2$ alone (A) and non-cycling holo-complex (B). **A.** Y• in $\beta_2$ alone: intrinsic lability (●) vs. decay in the presence of 3-AP (■). Representative experiment shown contained [(r-$His_6$-β)$_2$] = 5 μM, [3-AP] = 0 (●) or 50 (■) μM, 100 mM KCl in 50 mM Hepes (pH 7.6). (◆) in Fig. 2E represents the composite data where intrinsic decay has been adjusted. **B**. Y• in non-cycling holo-complex: in the absence (●) vs. presence (■) of 3-AP. Representative experiment contained [(r-$His_6$-α)$_2$] = [(r-$His_6$-β)$_2$] = 5 μM, [3-AP] = 0 (●) or 50 (■) μM, [ATP] = 3 mM, [$MgCl_2$] = 15 mM, 100 mM KCl in 50 mM Hepes (pH 7.6).

**Figure S2.**

**A**

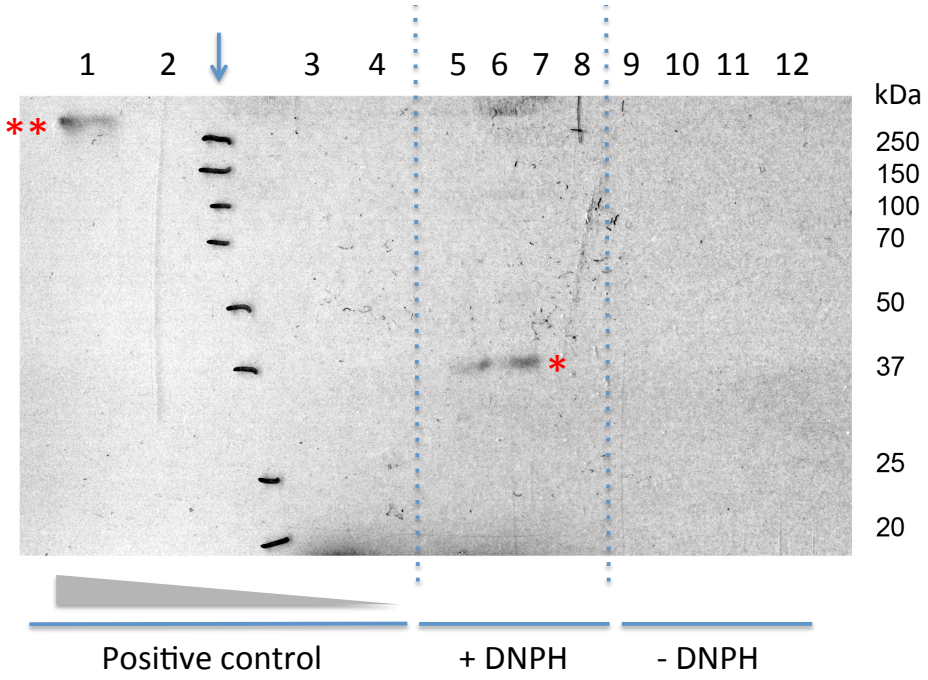
1 2 3 4 5 6 7 8 9 10 11 12
kDa
250
150
100
70
50
37
25
20
Positive control
+ DNPH
- DNPH

**B**

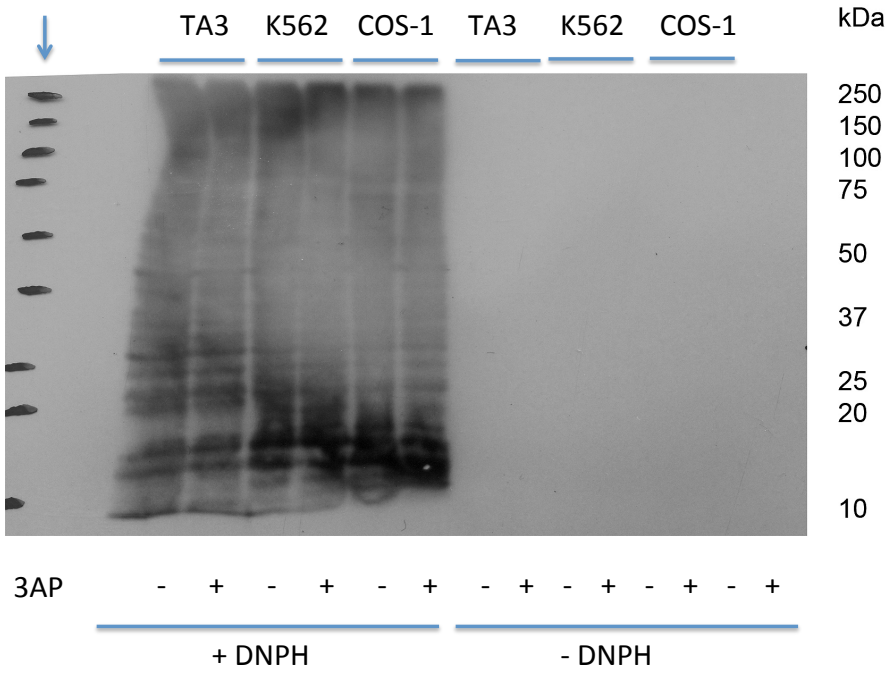
TA3 K562 COS-1 TA3 K562 COS-1
kDa
250
150
100
75
50
37
25
20
10
3AP - + - + - + - + - + - + - +
+ DNPH
- DNPH

**Figure S2.** Oxyblot analyses *in vitro* (A) and in lysates (B). **A.** *In Vitro* Oxyblot analysis of cycling holo-complex treated with 3-AP or DMSO (controls); samples were derivatized with DNPH (performed according to Millipore Oxyblot™ kit) and subsequently analyzed by SDS-PAGE and western blot. *Lanes 1-4*, Positive control (oxidized $\beta_2$) samples [5, 4, 3, 2 mg/mL of β (47 kDa monomer) was treated with excess iron and ascorbate; see SI Text for details]. ** likely indicates oxidatively-modified $\beta_2$ that presumably has undergone carbonylation and subsequent crosslinking. *Lanes 5-8*, Cycling holo-complex in Trx/TrxR/NADPH (lanes 5 & 6) in the presence of DMSO (lane 5) or 3-AP (lane 6), or in DTT (lanes 7 & 8) in DMSO (lane 7) or 3-AP (lane 8). * most likely corresponds to carbonylated TrxR based upon its MW (35 kDa). *Lanes 9-12*, Identical to lanes 5-8 except buffer replaced DNPH. Note that analogous *in vitro* Oxyblot analyses on $\beta_2$ alone or non-cycling holo-complex, with and without DNPH treatment in all cases, showed no western signals. In all cases, treatment of $\beta_2$ with 3-AP or DMSO was carried out under identical sets of conditions to those described in Fig. 2B-D ($\beta_2$ alone, non-cycling or cycling holo-complex), except in additional experiments wherein holo-complex undergoes turnover in the presence of 10 mM DTT instead of Trx/TrxR/NADPH (lanes 7 & 8). **B.** Oxyblot analyses in lysates. 5-50 μM 3-AP-treated and –untreated TA3, K562 and COS-1 cells, subsequent 0.5-3 h incubation with the inhibitor, were lysed and protein carbonyls in the lysate were derivatized with DNPH. Representative data shown is from 3 h treatment with 50 μM 3-AP.

**Figure S3.**

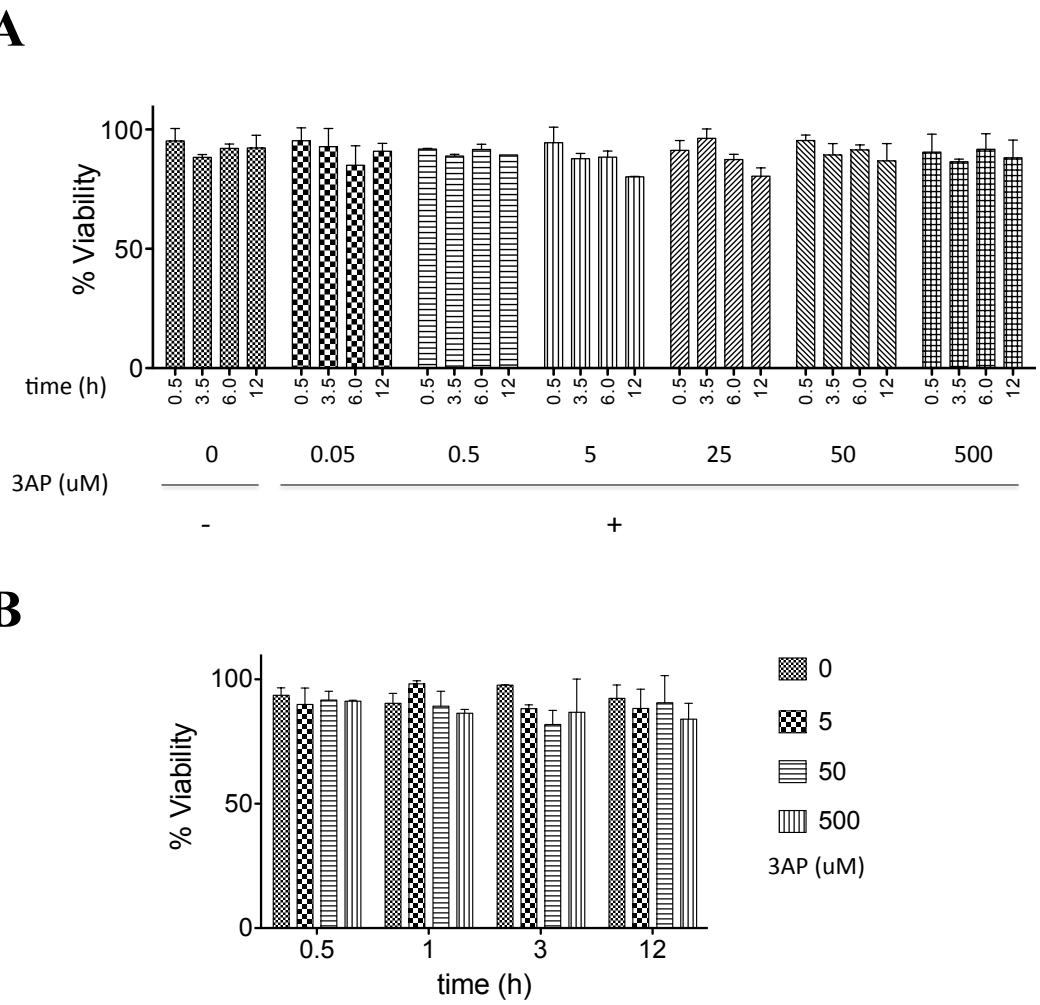


**Figure S3.** Cell viability over a range of 3-AP concentrations and incubation periods analyzed by trypan blue assay. Representative data from COS-1 (**A**) and K562 (**B**) cells. Error bars correspond to SD over duplicate experiments.

**Figure S4.**

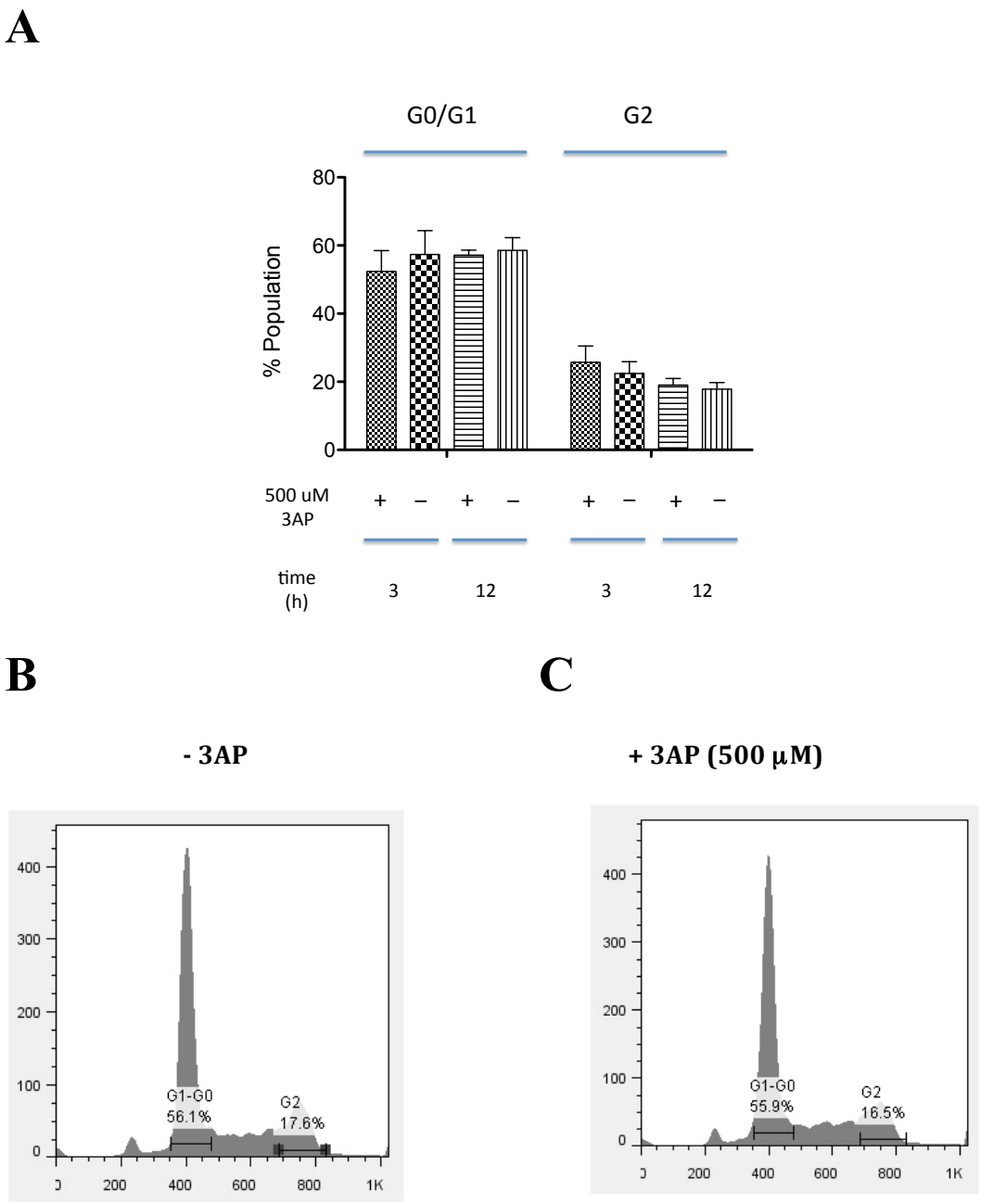


**Figure S4.** Representative data from FACS analysis. 3-AP-treated and -untreated cells were fixed, subjected to PI-staining and analyzed by flow cytometry. **A**. Results with COS-1 cells treated with 500 µM 3-AP at 3 or 12 h exposure. Error bars are SD from duplicate sets of cultures. **B-C**. Representative histograms from the untreated (**B**) and treated (**C**) COS-1 cells at 12 h exposure to 500 µM 3-AP.

**Figure S5.**

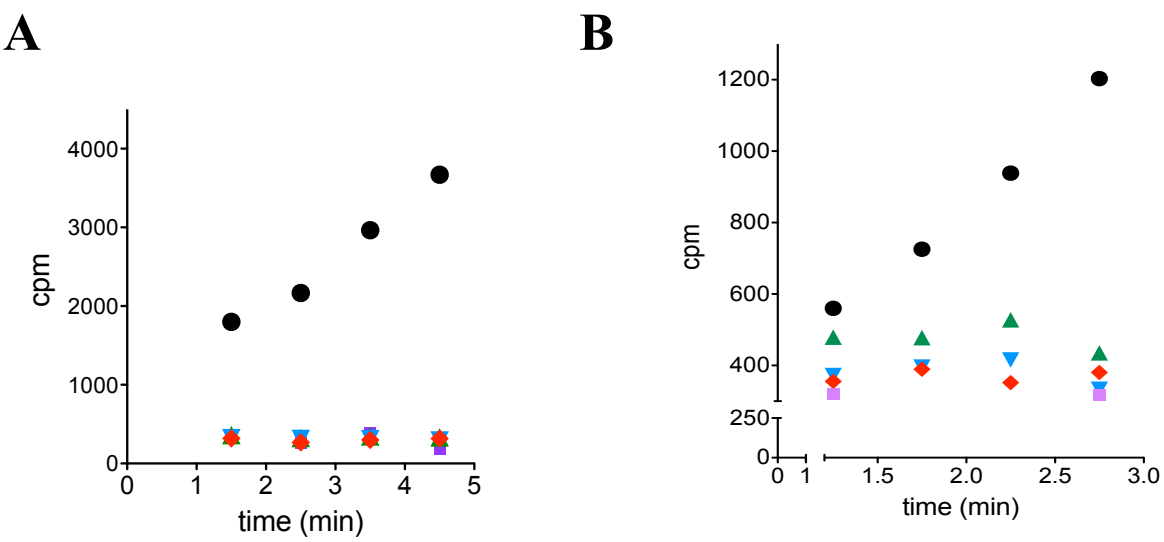


**Figure S5.** Depletion of $\beta_2$- activity in lysates from 3-AP treated (30 min) (A) COS-1 and (B) K562 cells. Total lysate protein amount in each experiment, as estimated by Bradford assays, was 0.2 and 0.05 mg, respectively. [3-AP]= 0 (●), 5 (▼), 50 (◆), 500 (▲) μM; background (■). Also see Fig. 3A.

**Figure S6.**

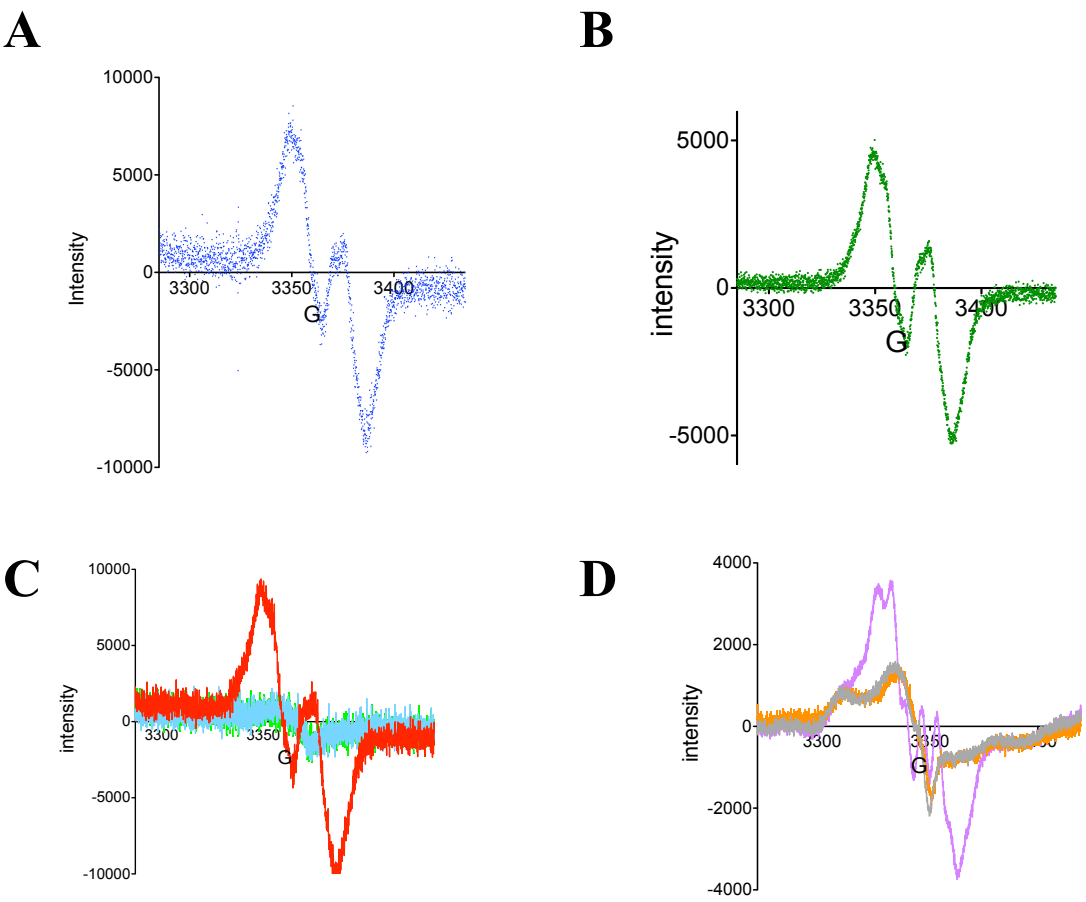


**Figure S7.** Whole cell EPR analysis of Y• in 3-AP-treated and untreated cells. **A**. HU-resistant TA3 cells with endogenous Y• signal. Spectrum was acquired at 77 K (10 scans), using ~80x10$^6$ intact TA3 cells (Cf. Fig. 3B, data collected at 30 K). **B**. For comparison, recombinant holo-$\beta_2$ reconstituted *in vitro* is shown. Spectrum was acquired at 77K (10 scans) for 59 μM (r-His$_6$-β)$_2$, with 1.0 ± 0.1 Y•/$\beta_2$. **C**. Y• signal in 3-AP-treated (0.5 h) (••• 5 or ••• 50 μM) and untreated (•••)~80x10$^6$ intact TA3 cells. Spectra acquired at 77 K. See Fig. 3B for corresponding data after 3 h treatment. **D**. Y• signal in 3-AP-treated (0.5 h) (••• 5 or ••• 50 μM) and untreated (•••)~80x10$^6$ intact K562 cells. Spectra acquired at 30 K. Note that endogenous Y• in K562 cells was not observable at 77 K due to poor signal:noise.

**Figure S7.**

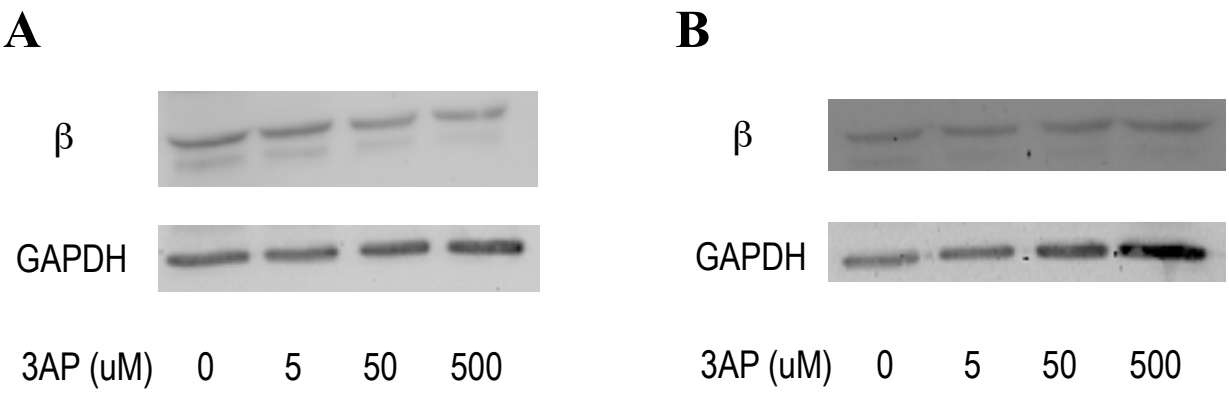


**Figure S7.** Maintenance of $\beta_2$ protein levels in 3-AP-treated (**A**) COS-1 and (**B**) TA3 cells. Treated and untreated cells were harvested and lysed at 30 min incubation time point. See Fig. 4C for analogous data with TA3 cells. GAPDH was used as the loading control.

## SUPPLEMENTAL TABLE

**Table S1**

| **% Coverage:** | Control | Sample 1 | Sample 2 |
|---|---|---|---|
| | 67% | 54% | 68% |

**Table S1A. Modification: Oxidation (Any Residue)**

| Entry | Peptide sequence | Control | | Sample 1 | | Sample 2 | |
|---|---|---|---|---|---|---|---|
| | | Non-ox | ox | Non-ox | ox | Non-ox | ox |
| 1 | (K)DIQH**W**ESLKPEER(Y) | | X | X | | | X |
| 2 | (R)EFLFNAIET**M**PCVK(K) | | X | | X | | X |
| 3 | (R)FVIFPIEYHDIWQ**M**YK(K) | | X | X | | | X |
| 4 | (K)KAD**W**ALR(W) | | X | X | | | X |
| 5 | (R)L**M**LELGFS(K) | | X | X | | | X |
| 6 | (K)LIG**M**NCTL**M**K(Q) | | X | | X | | X |
| 7 | (K)VFRVENPFDF**M**ENISLEGK(T) | | X | | X | | X |
| 8 | (R)GL**M**PGLTFSNELISR(D) | | X | | X | | X |
| 9 | (K)KAEASF**W**TAEEVDLSK(D) | X | | X | | | X |

**Table S1B. Modification: Hydroxylation (Y or F)**

| Entry | Peptide sequence | Control | | Sample 1 | | Sample 2 | |
|---|---|---|---|---|---|---|---|
| | | Non-hy | hy | Non-hy | hy | Non-hy | hy |
| 1 | (K)TNF**F**EKR(V) | | X | | X | | X |
| 2 | (K)Q**Y**IEFVADR(L) | | X | | X | | X |
| 3 | (R)IEQE**F**LTEALPVK(L) | X | | X | | | X |

**Amino acid sequence for hRNR β.**

MLSLRVPLAPITDPQQLQLSPLKGLSLVDKENTPPALSGTRVLASKTARRIFQEPTEPKTKAAAPGVEDEPLL
RENPRRFVIFPIEYHDIWQMYKKAEASFWTAEEVDLSKDIQHWESLKPEERYFISHVLAFFAASDGIVNENL
VERFSQEVQITEARCFYGFQIAMENIHSEMYSLLIDTYIKDPKEREFLFNAIETMPCVKKKADWALRWIGDK
EATYGERVVAFAAVEGIFFSGSFASIFWLKKRGLMPGLTFSNELISRDEGLHCDFACLMFKHLVHKPSEERV
REIIINAVRIEQEFLTEALPVKLIGMNCTLMKQYIEFVADRLMLELGFSVENPFDFMENISLEGKTNFFEKRV
GEYQRMGVMSSPTENSFTLDADF

**Table S1.** Trypsin digest LCMS analysis of 5 μM (r-$His_6$-β)$_2$ treated *in vitro* at 37 °C for 20 min with 50 μM of either Fe(II)-(3-AP) (Sample 1) or $H_2O_2$ (Sample 2). DMSO was used for Control. **A.** Oxidative side-chain modifications of resulting peptides from the three samples. Amino acids in **Red** designate oxidatively modified residues. Ox, oxidized. **B.** Y and F hydroxylation in the three samples. **Blue** aa's correspond to hydroxylated (hy) residues. In both tables, parenthesized amino acids are not part of the sequence but indicate trypsin cleavage sites. Sequence of hRNR β is shown. See SI Text for a detailed procedure and analysis.